

# The C-terminus of prestin influences nonlinear capacitance and plasma membrane targeting

Jing Zheng<sup>1,\*</sup>, Guo-Guang Du<sup>1</sup>, Keiji Matsuda<sup>1</sup>, Alex Orem<sup>1</sup>, Sal Aguiñaga<sup>1</sup>, Levente Deák<sup>1</sup>, Enrique Navarrete<sup>1</sup>, Laird D. Madison<sup>2</sup> and Peter Dallos<sup>3</sup>

<sup>1</sup>Auditory Physiology Laboratory, Department of Communication Sciences and Disorders, Northwestern University, Evanston, IL 60208 USA

<sup>2</sup>Feinberg School of Medicine, Northwestern University, Division of Molecular Medicine, Metabolism, and Diabetes, Chicago, IL 60611, USA

<sup>3</sup>Department of Neurobiology and Physiology, The Neuroscience Institute, Northwestern University, Evanston, IL 60208, USA

\*Author for correspondence (e-mail: jzh215@northwestern.edu)

Accepted 7 April 2005

Journal of Cell Science 118, 2987-2996 Published by The Company of Biologists 2005

doi:10.1242/jcs.02431

## Summary

Prestin is a unique molecular-motor protein expressed in the lateral plasma membrane of outer hair cells (OHC) in the organ of Corti of the mammalian cochlea. It is thought that prestin undergoes conformational changes driven by the cell's membrane potential. The resulting alterations in OHC-length are assumed to constitute the cochlear amplifier. Prestin is a member of the anion solute carrier family 26 (SLC26A), but it is different from other family members in its unique function of voltage-driven motility. Because the C-terminus is the least conserved region in the family, we investigated its influence with a series of deletion, point and chimeric mutants. The function and cellular expression of mutants were examined in a heterologous expression system by measurement of nonlinear capacitance (NLC) and immunofluorescence. Each mutant produced a unique mixture of patterns of cell morphologies, which were classified as to the location of prestin within the cell. The data from deletion mutants (Del516, Del525, Del630, Del590, Del709, Del719) revealed that nearly the full length (>708 amino acids) of the protein was required for normal prestin expression and function.

Since most deletion mutations eliminated plasma membrane targeting, chimeric proteins were constructed by fusing prestin, at amino acid 515 or 644, with the homologous portion of the C-terminus from the two most closely related SLC26A members, pendrin and putative anion exchanger 1. These chimeric proteins were again improperly (but differently) targeted than simple truncation mutants, and all lacked functional phenotype. When two of the potential basolateral membrane-targeting motifs were mutated (Y520A/Y526A), incomplete plasma membrane expression was seen. We also show that some double point mutations (V499G/Y501H) fully express in the plasma membrane but lack NLC. These non-charged amino acids may have unrevealed important roles in prestin's function. Together, these data suggest that certain specific sequences and individual amino acids in the C-terminus are necessary for correct cellular distribution and function.

Key words: Prestin, Outer hair cells, C-terminus, STAS, Nonlinear capacitance, Membrane targeting

## Introduction

The mammalian cochlea is a highly complex, sensitive sensor and amplifier of acoustic input. The organ of Corti, the site of acoustic energy transduction, contains two sensory types of hair cells: (1) inner hair cells, which receive ~95% of the afferent innervation of the cochlea and are the true sensory receptor cells, and (2) outer hair cells, which receive dominant efferent innervation and are responsible for the sensitivity and frequency selectivity of mammalian hearing by providing local mechanical amplification (Dallos, 1992; Dallos, 1996). These cells undergo rapid length changes in response to their receptor potentials (Ashmore, 1987; Brownell et al., 1985; Kachar et al., 1986). These changes in outer hair cell length are thought to feed back energy within the organ of Corti, thereby amplifying the mechanical input signal ~50-60 dB to the adjacent sensory inner hair cells. The length changes are mediated by the motor protein, prestin, located in the lateral membrane of the cylindrical OHC (Zheng et al., 2000). This action of prestin on OHC length is dependent on the OHC membrane potential, and can take place in the absence of ATP,

Ca<sup>2+</sup>, or even a cytoskeletal structure (Holley, 1996). Deletion of prestin has been shown to result in the loss of ~40-60 dB in hearing sensitivity in mice (Liberman et al., 2002) and elimination of frequency selectivity (Cheatham et al., 2004). A human prestin mutation has also been identified, showing severe hearing impairment (Liu et al., 2003).

Prestin is a member of the SLC26A anion-transport family (Mount and Romero, 2004). It is also related by homology to an ancient family of hydrophobic membrane anion transporters, SulP, ubiquitously expressed in eukaryotes, prokaryotes and plants (Loughlin et al., 2002; Saier, 1999). Ten mammalian members of the SLC26A family have been identified. All of these members have common structural features: a highly conserved central core of hydrophobic amino acids, forming 10-14 transmembrane domains and a long cytoplasmic C-terminus. The SLC26A 'sulfate transporter signature' is present in the second transmembrane domain, while a STAS (sulphate transporter and antisigma-factor antagonist) motif (Zheng et al., 2001) is located in the C-terminal tail (amino acids 634-710 for prestin). In contrast to

the highly conserved hydrophobic core, the intracellular C-terminus of prestin only has 25-35% homology with its other SLC26A relatives.

SLC26A proteins produce significant human diseases when altered. Severe hearing deficit can result from mRNA splicing mutation of the *PRES* gene (Liu et al., 2003). Pendred's syndrome results from mutation of the *PDS* (Pendred's syndrome) gene (Everett and Green, 1999; Everett et al., 1999; Scott et al., 2000; Soleimani et al., 2001). Familial chloride diarrhea is the result of the mutation of the *DRA* (down-regulated in adenoma) gene (Kere et al., 1999). A variety of distinct skeletal diseases, such as multiple epiphyseal dysplasia, are a consequence of mutations of the *DTDST* (diastrophic dysplasia sulfate transporter) gene (Hastbacka et al., 1996a; Hastbacka et al., 1996b; Superti-Furga et al., 1996a; Superti-Furga et al., 1996b; Superti-Furga et al., 1996c). The majority of the disease-causing mutations in *PDS*, *DRA* and *DTDST* are located in the hydrophobic transmembrane segment of the proteins, but about a third occur in the less well-conserved C-termini. Analysis of the mutations in Pendred's syndrome has revealed that many C-terminus mutants result in impaired membrane targeting and retention of the protein in intracellular compartments (Rotman-Pikielny et al., 2002; Taylor et al., 2002).

All members of the SLC26A family, except prestin, transport biological anions ( $\text{SO}_4^{2-}$ ,  $\text{I}^-$ ,  $\text{Cl}^-$ ) across the plasma membrane. To date, prestin appears to behave as an incomplete anion transporter, as no anion transport has been correlated with its function (Dallos and Fakler, 2002), although some data suggested that it can transport sugar instead (Chambard and Ashmore, 2003). Prestin utilizes intracellular  $\text{Cl}^-$  ions as extrinsic voltage sensors for promoting charge translocation (Oliver et al., 2001; Rybalchenko and Santos-Sacchi, 2003). After binding to prestin,  $\text{Cl}^-$  anions are partially translocated across the membrane in response to changes in the

transmembrane voltage. This translocation is assumed to trigger conformational changes in the molecule, resulting in an increased (or decreased) membrane area, and elongation (or contraction) of cells. Prestin demonstrates voltage-dependent charge transfer, manifested as nonlinear capacitance (Ashmore, 1990). NLC is a result of a gating current, a charge dislocation across the cell membrane, which is commonly accepted as a signature of motor action (Santos-Sacchi, 1991). How the membrane-potential change of OHCs results in structural changes in prestin, corresponding to the motor function, is not understood. Other members of the SLC26A family, such as *PDS* (SLC26A4) and *PAT1* (putative anion exchanger 1, SLC26A6), do not show NLC under similar conditions (Oliver et al., 2001; Zheng et al., 2000).

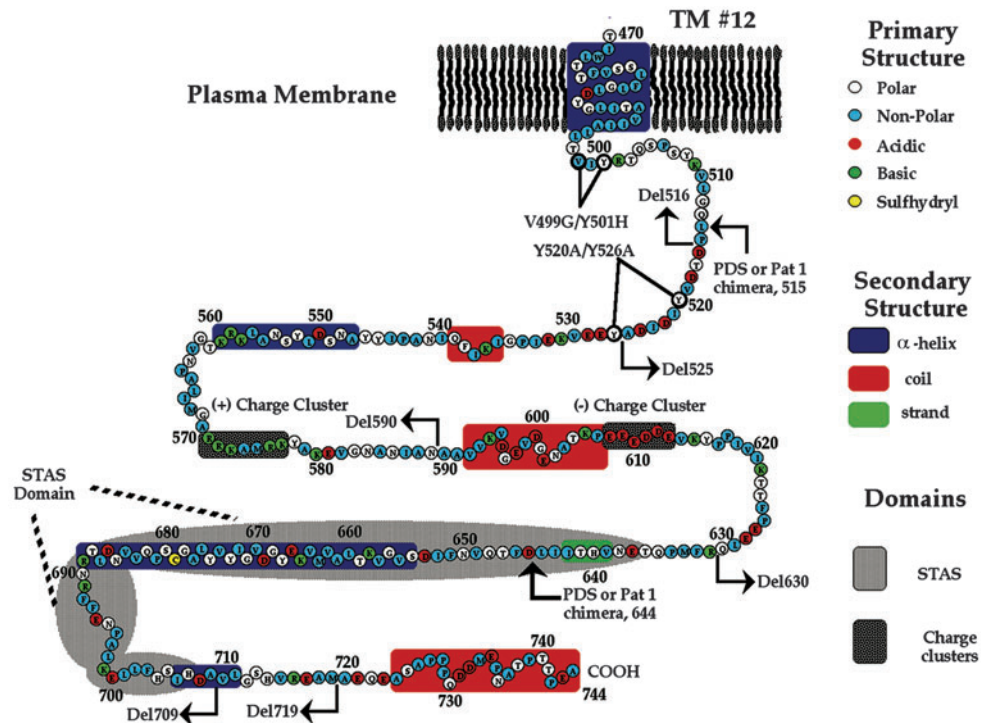
Since the C-terminus is the least conserved region of the protein among different SLC26A family members, we reasoned that it is most likely to be responsible for each SLC26A protein's specific function. The detailed sequence of prestin's C-terminus and its putative secondary structure as predicted by PSIPRED (The PSIPRED Protein Structure Prediction Server) (Jones, 1999; McGuffin et al., 2000) are shown in Fig. 1. Our approach towards determining the mechanism of prestin's motor action is to establish correlations between prestin function and the role of specific domains in the C-terminus. We used serial deletions, site-directed mutagenesis, and chimeric proteins to study the role of the C-terminus of prestin. Mutant-protein behavior was examined using both NLC and intracellular protein distribution by immunofluorescence.

## Materials and Methods

### Antibodies

Rabbit anti-NH2 terminus mPres (anti-N-mPres) polyclonal antibody (Ab) was raised by immunization with a synthetic oligopeptide

**Fig. 1.** A secondary structure and topology model of prestin's C-terminus based on a topological model previously described (Zheng et al., 2000). The properties of the amino acids side chains are indicated by different colors for polar (clear), non-polar (blue), acidic (red), basic (green) and cysteine residues (yellow) moieties. The location of the last transmembrane domain is based on the program TMPRED (transmembrane predictions). Regions of the C-terminus with a predicted secondary structure using the program PSIPRED (confidence  $\geq 6-9$ ) are indicated by colored backgrounds;  $\alpha$ -helix (blue), coil (red), and strand (green). The STAS domain (gray), and charge clusters (speckled) are indicated by background shading. The locations of the mutations created in prestin mutant proteins examined in this study are indicated with arrows in the cartoon. These include deletion mutants, chimera junction points and double point mutations.



corresponding to the amino terminus motif of mouse prestin, MDHAEENEIPAETQRYYYVER. Characterization of this antibody demonstrated that it functioned similarly to anti-N-gprestins, which has been previously characterized (Zheng et al., 2001). ELISA, western blot and immunofluorescence experiments performed on prestin-expressing samples were used to test the specificity of this antibody. Anti-N-mPres, was used in a 1:2000 dilution in immunofluorescence experiments. Na<sup>+</sup>/K<sup>+</sup> ATPase and Golgin 97 are a plasma membrane protein and a Golgi marker, respectively. Anti-Na<sup>+</sup>/K<sup>+</sup> ATPase (10 ng ml<sup>-1</sup>, Upstate Biotechnology, Lucerne) was used as a plasma membrane protein marker and anti-Golgin 97 (1:200 dilution, Molecular Probes, Eugene, OR) as a Golgi marker. Anti-Flag (1:1000 dilution, Sigma) was used to detect GHRH (growth hormone releasing hormone) receptor, which is a plasma membrane protein. Secondary antibodies, FITC conjugated anti-rabbit IgG and Rhodamine conjugated anti-mouse IgG were purchased from Pierce (Rockford, IL) or Jackson Immuno Research (Bar Harbor, ME).

### DNA constructs and mutagenesis

Gerbil prestin (gprestins) cDNA was cloned into pcDNA3.1 (Zheng et al., 2000) and pEGFP-N2, the latter of which generates a gprestins-EGFP fusion protein with EGFP (Enhanced green fluorescent protein) attached to the C-terminus of prestin. The double point mutations V499G/Y501H and Y520A/Y526A were generated using a QuickChange Site-Directed Mutagenesis Kit (Stratagene, Cedar Creek, TX). The nucleotide exchanges were confirmed by DNA sequencing. The deletion mutants: Del525-744 (Del525), Del590-744 (Del590), Del630-744 (Del630), Del709-744 (Del709) and Del719-744 (Del719) were generated by PCR or restriction enzyme digestion and re-ligation of wild-type gprestins cDNA. Del516-744 (Del516) was generated in mouse prestin (mprestins) cDNA to utilize a unique restriction site. The chimeric protein PRES/PDS-515 was constructed with amino acids 1-515 of gerbil prestin and amino acids 525-780 of human PDS. The PRES/PAT1-515 chimera was constructed with amino acids 1-515 from gerbil prestin and amino acids 499-738 from human PAT1. PRES/PDS-644 consisted of amino acids 1-644 of gerbil prestin, and amino acids 660-780 of human PDS, while PRES/PAT1-644 contained amino acids 1-644 of gerbil prestin and amino acids 652-738 of human PAT1. The plasmid pcDNA3.1-CAT (Choramphenicol acetyl-transferase) was used as a transfection control in the expression studies.

### Cell culture and transient transfection

Prestin and mutant plasmids were transiently expressed in TSA-201 cells, a sub-clone of human embryonic kidney 293 cells, or in opossum kidney (OK) cells. TSA-201 cells were cultured as described previously (Zheng et al., 2001). For OK cells, MEM Eagle was used, supplemented with 10% fetal bovine serum, 1 mM sodium pyruvate, 1× Non-Essential Amino Acid (GiBco, Carlsbad, CA), 0.075% sodium bicarbonate in addition to 100 U ml<sup>-1</sup> penicillin, and 100 µg ml<sup>-1</sup> streptomycin. Both cells were transiently transfected using Effectene (Qiagen, Valencia, CA) as the transfection reagent as described previously (Matsuda et al., 2004). In some experiments, the prestin construct was co-transfected with an enhanced green fluorescence protein cDNA expressing plasmid pEGFP-N2 (Clontech, Palo Alto, CA) in 10:1 ratio. This plasmid generates cytoplasmic EGFP protein as an independent marker for successful transfection of individual cells and for determination of a cytoplasmic protein immunofluorescence pattern. After 24-48 hours incubation, the transfected cells were used for immunofluorescence or NLC measurement. In some cases, a cDNA plasmid expressing the GHRH receptor was co-transfected with prestin or prestin mutant plasmids in 1:1 ratio. The GHRH receptor, kindly provided by K. Mayo, is a well-characterized G-protein-coupled receptor located in the plasma membrane (PM).

## Immunofluorescence experiments

### Cell culture

The procedure for immunofluorescence experiments has been described in detail before (Zheng et al., 2001). Briefly, the transiently transfected cells were fixed with 1% formaldehyde in PBS for 10 minutes at room temperature at 24 or 48 hours after transfection. The cells were incubated with anti-N-mPres, anti-Na<sup>+</sup>/K<sup>+</sup> ATPase, anti-Golgin 97, or anti-Flag in PBS with 5% BSA, and 0.1% saponin. Secondary antibodies, anti-mouse IgG or anti-rabbit IgG, conjugated with different fluorescent labels, were incubated in PBS with 5% BSA, 0.1% saponin and 10% normal donkey or goat serum. The samples were mounted on glass slides with Fluoromount-G (Southern Biotechnology Associates, Inc., Birmingham, AL) and observed using a Leica confocal system with a standard configuration DMRXE7 microscope.

### In vivo

All surgical and experimental procedures were conducted in accordance with the policies of Northwestern University's Animal Care and Use Committee. Adult Mongolian gerbils, mice and prestin knockout mice (kindly provided by J. Zuo) were cardiac perfused first with heparinized saline and then with 4% formaldehyde. After ~4 hours post fixation in 4% formaldehyde at room temperature, cochleae were dissected, decalcified overnight in 10% EDTA and treated with 0.3% Triton X-100/PBS. Ovalbumin was used to block nonspecific binding. The tissue samples were then exposed to the anti-N-mPres antibody similar to the procedure for the cell culture immunolabeling as described above.

### Whole cell recordings in TSA-201 cells

Voltage-dependent capacitance was measured 48-72 hours after transient transfection with prestin or its associated mutant constructs into TSA-201 cells or OK cells. Cells were isolated for measurements using a non-enzymatic cell dissociation agent (Sigma-Aldrich, St Louis, MO). Cells were selected for measurement based on the presence of a co-transfected positively expressed EGFP marker. Whole-cell patch-clamp recordings were performed using the Axopatch 200B amplifier (Axon Instruments, Foster City, CA) at room temperature. Recording pipettes were pulled from borosilicate glass to achieve initial bath resistances of 1.5-3.0 MΩ and filled with a solution containing (mM): 140 CsCl, 2 MgCl<sub>2</sub>, 10 EGTA, and 10 HEPES. The cells were bathed during whole-cell recordings in a solution containing (mM): 120 NaCl, 20 TEA-Cl, 2 CoCl<sub>2</sub>, 2 MgCl<sub>2</sub>, 10 HEPES, 5 glucose. Both solutions were adjusted to pH 7.2 and the osmolarity was adjusted to 300 mOsm<sup>-1</sup>. Recording-chamber perfusion was continuous during whole-cell measurements. Data collection was performed using the software jClamp (SciSoft Company, New Haven, CT). Membrane capacitance is measured by AC analysis using a software-based lock-in amplifier technique. A dual sinusoidal voltage stimulus protocol, with amplitudes of 10 mV peak and frequencies of 390.6 and 781.2 Hz, was applied to the membrane and current amplitude and its phase were computed. The linear or voltage-independent membrane capacitance component is proportional to cell surface area. Prestin-expressing cells exhibit a membrane capacitance composed of voltage-independent and voltage-dependent capacitance components [ $C_m=C(V)+C_{lin}$ ] (Ashmore, 1990; Rybalchenko and Santos-Sacchi, 2003; Santos-Sacchi, 1991). The voltage-dependent, or nonlinear capacitance (NLC), is described by the voltage-derivative of a first order Boltzmann function relating charge movement and voltage:

$$C_m(V) = C_{lin} + \frac{Q_{max}}{\alpha e^{\left(\frac{V-V_{1/2}}{\alpha}\right)} \left(1 + e^{-\left(\frac{V-V_{1/2}}{\alpha}\right)}\right)^2}, \quad (1)$$

where  $Q_{max}$  is maximum charge transfer,  $V_{1/2}$  is the voltage at which the maximum charge is moved across the membrane,  $C_{lin}$  is the linear capacitance of the cell, and  $\alpha = ze/kT$  is the slope factor of the voltage dependence of charge transfer where  $k$  is Boltzmann's constant,  $T$  is absolute temperature,  $z$  is the valence and  $e$  is electron charge. IGOR Pro (Wavemetrics, Lake Oswego, OR) was used for fitting the NLC with the derivative of the first order Boltzmann function.

## Results

### Functional analysis of truncation mutants measured by NLC

The unique property of prestin is its ability to confer NLC and motility to heterologous cells (Zheng et al., 2000). We deleted progressively larger portions of the C-terminus of prestin and examined the effect of these truncations on the NLC of cells expressing the deletion-mutants. The following set of C-terminal truncation mutants examined in this study (Fig. 1) retained various portions of the C-terminus: Del516, Del525,

Del590, Del630, Del709 and Del719. Del516 and Del525 were generated from mouse prestin and gerbil prestin respectively, and eliminate the majority of the C-terminus, while Del590 truncates the protein before the negative charge cluster region. Del630 retains both positive and negative charge regions, but lacks the STAS motif. Del709 contains the STAS domain, while Del719 lacks only the terminal 25 amino acids of prestin. Each of the mutant constructs illustrated in Fig. 1 were transfected into TSA-201 or OK cells and their electrophysiology examined in a minimum of 12 cells each in two separate experiments for each mutant form.

The NLC of each of the C-terminus deletion mutants, except Del719, was completely abolished. The electrophysiological profile of the NLC of Del719 was similar to wild-type prestin as shown in Fig. 2. The figure shows examples for the representative NLC patterns for deletion-constructs, double point mutations, positive (wild type), and negative controls (NLC signature for untransfected cells). Included in Fig. 2 is the capacitance function for Del709, which is representative of results obtained for all deletion mutant constructs, including Del516, Del525, Del590, Del630 and Del709. In addition, the figure shows the results for the mutant Y520A/Y526A. For comparison, the NLC pattern for an untransfected cell is also provided to show that there is no difference between the function of these mutants and that of untransfected cells. Comparing these functions to that of a positive control cell (wild type), the data demonstrates that these cells do not exhibit NLC function. Fig. 2b shows on an expanded ordinate scale the capacitance of those cells in Fig. 2a that had negligible NLC. Conversely, the Del719 construct exhibited a voltage-dependent capacitance, not unlike wild type. Statistical tests of differences between Del719 and wild-type (wt) prestin reveal that none of the curve-fitting parameters are different. For example, the  $t$ -test yields  $P=0.75$  for the charge density parameter. These data were obtained, as our usual procedure, by comparing groups of cells (wild type versus mutant) transfected and tested on the same day. To clarify our procedures, note that NLC from 10–12 cells were measured for any condition. In those cases where an NLC function could be fitted (wild type and Del719), the fit parameters (Eqn 1) were obtained for each cell. These parameters describe the entire curve, i.e. the behavior of capacitance as a function of membrane potential. The central tendency of all fit parameters for the population of cells was computed, as well as the  $t$ -tests to examine differences, if any. Plots in Fig. 2 are for those individual cells that best reflect the mean of the appropriate population.

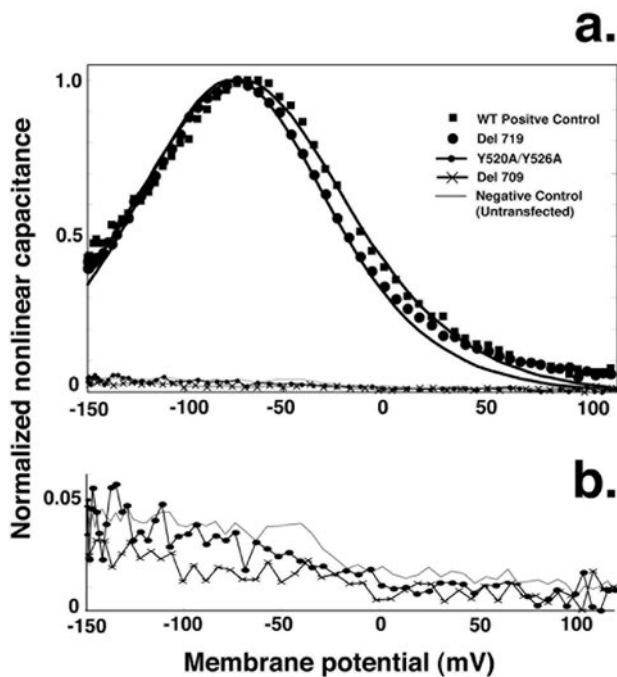


**Fig. 2.** (a) Voltage-dependent membrane capacitance of TSA-201 cells transiently transfected with wild type (positive control), Del719, Del709, Y520A/Y526A, as well as untransfected cells (negative control). All capacitance plots are normalized to the maximum of the corresponding (same transfection, same experiment) wild-type NLC function. (b). Membrane capacitance for constructs Del709, Y520A/Y526A, and a negative control plotted relative to their minimum capacitance value. The capacitance waveforms for these constructs are relatively flat and similar to the negative control. The voltage at the peak of the capacitance function represents most efficient charge transfer, while the peak itself relates to the amount of charge translocated. The double point mutation Y520A/Y526A and Del709 mutants exhibited no measurable NLC, whereas the Del719 mutation has normal capacitance relative to wild-type control cells from the same transfection batch. NLC measurements are analyzed by extracting parameters that describe the cell's  $Q_{max}$ ,  $\alpha$ ,  $V_{1/2}$  and  $C_{lin}$ . The parameters are obtained from measurements where the voltage range was between  $-150$  mV and  $+120$  mV. The individual plots shown are representative of the average parameters ( $n > 10$ ).

### Cellular distribution of prestin and its mutant isoforms

Prestin is a membrane-spanning protein in the lateral plasma membrane of OHCs. Because of the loss of function in all but the shortest of the prestin truncations, we examined the cellular expression patterns of transiently expressed prestin mutants using confocal immunofluorescence imaging in TSA-201 and OK cells. To study the location of prestin in transiently transfected cells, we raised an anti-N-mPres antibody against an epitope comprising the first 20 amino acids at the 5'-terminus of mouse prestin. This antibody is similar to the anti-N-gprestin that we have made and used before (Zheng et al., 2001). The specificity of anti-N-mPres is demonstrated in Fig.

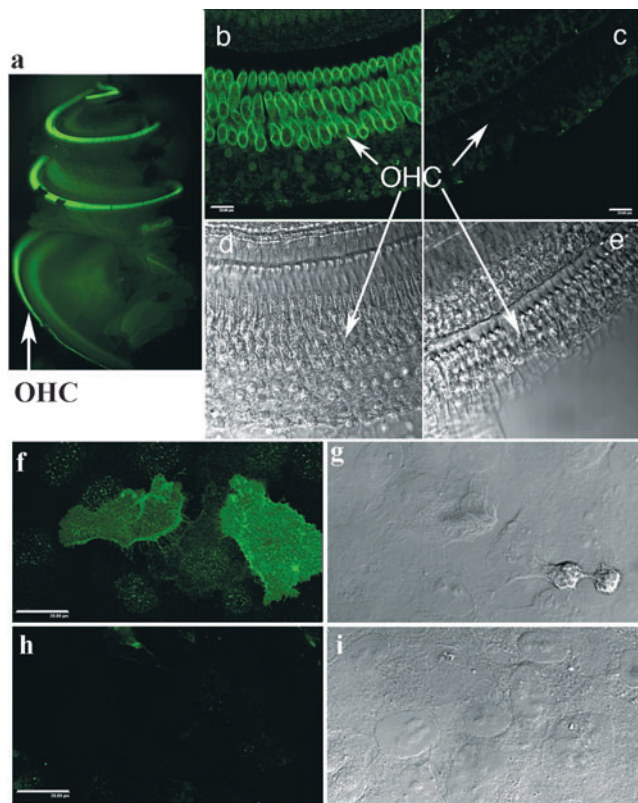


**Fig. 3.** Characterization of anti-N-mPres. (a) Immunofluorescence image of a gerbil cochlea stained with anti-N-mPres. The low-magnification image is taken with an epifluorescent microscope with 25 $\times$  objective. The high-magnification images of OHCs are obtained by confocal microscopy, these are shown in b-e.

Immunofluorescence and corresponding phase-contrast images of a normal gerbil (b and d) are compared with material obtained from a prestin knockout mouse (c and e). Both wild-type gerbil and prestin knockout cochlea samples are stained with anti-N-mPres.

(f,g) Immunofluorescence and corresponding phase-contrast images of OK cells transiently transfected with wild type, then stained with anti-N-mPres. (h,i) Immunofluorescence and corresponding phase-contrast images of OK cells transiently transfected with the control vector pcDNA3.1-CAT. Bar, 20  $\mu$ m.

3. Anti-N-mPres specifically stained the three rows of OHCs in the entire gerbil cochlea (Fig. 3a). Similar results were also obtained from wild-type mouse cochlea. Because most of the prestin mutants were made from gerbil prestin cDNA, we have chosen to present images of gerbil cochlea instead of those of the mouse. At high magnification, prestin is clearly seen to be located in the lateral membrane of OHC (Fig. 3b,d), but not in OHCs obtained from a prestin knockout mouse (Fig. 3c,e), in agreement with previous reports (Belyantseva et al., 2000; Zheng et al., 2001). In prestin-transfected OK or TSA-201 cells, only transfected cells showed staining as demonstrated in Fig. 3f,g. Cells transfected with the negative control vector pcDNA3.1-CAT did not show fluorescent staining as expected (Fig. 3h,i). Images of OK cells were used for analysis instead of TSA-201 cells because their morphology, with a larger cytoplasm-to-nucleus ratio, allowed for better determination of intracellular localization. NLC measurements for wild-type prestin expressed in either TSA-201 cells or OK cells were

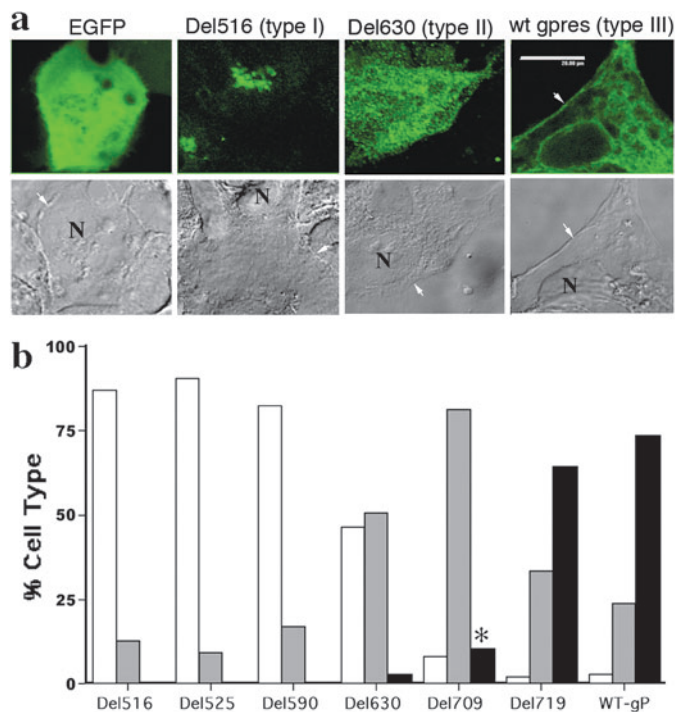


**Fig. 4.** Representative patterns of wild-type prestin and associated deletion mutants transfected into OK cells. (a) Immunofluorescence and corresponding phase-contrast images of OK cells transiently transfected with cytoplasmic protein EGFP, deletion mutant examples showing types I, and II morphology, and wild type (wt), representing type III morphology. All samples were stained with FITC-labeled anti-N-mPres, except the EGFP preparation. Cell boundaries are marked by arrows. 'N' stands for nucleus. Bar, 20  $\mu$ m. (b) Distribution of the frequency of occurrence of the three cell types for different mutations 48 hours after transfection. The prestin-expressing cells in different samples were classified as types I, II and III, according to the location of prestin (see text); white bars indicate type I, gray bars type II, and black bars type III cells. We note here that some cells classified as type III, found in the Del709 mutant (\*), were actually found not to be so after testing for co-localization with the PM marker as described in Fig. 5 (also see text).

similar (data not shown). Each transfection produced different prestin expression patterns in different cells in the same culture dish. To characterize these patterns, we subjectively classified individual cells into three different types. Type I cells were characterized by dense, punctate, or linear staining mostly in the perinuclear region of the cell. Type II cells were defined as those displaying dense perinuclear staining as well as intracellular membranous staining without plasma membrane delineation. Type III cells, defined as wild type, demonstrated PM co-localization with variable degrees of intracellular membranous, and perinuclear labeling. Examples of types I-III are shown in Fig. 4a. The locations of nuclei for the cells in the images are labeled with 'N'. The arrows indicate the boundary of the cells. OK cells, transfected with the cytoplasmic protein marker EGFP construct alone, were used as a negative control. Unlike the vesicular and membranous-staining observed in type I, II and III cells, EGFP-expressing cells showed diffuse green fluorescent staining throughout the cytoplasm, as expected. The different prestin truncation mutants demonstrated different ratios of the three cell-

classification types. To quantify these observations, we subjectively graded the cells (approximately 100 cells for each experiment) by blind classification of cells from random immunofluorescence images from at least two transfection experiments for each truncated form of prestin 48 hours after their transfections. As shown in Fig. 4b, cells expressing Del516, Del525, and Del590 had a majority of type I pattern, approximately 10-20% type II phenotype, and no or very few type III cells. Del630 displayed a greater degree of phenotypic variation than the other mutants, with nearly equal amounts of types I and II patterns, and a small percentage of type III cells. Del709 produced a majority of cells with a type II distribution. Del719 resulted in a predominance of type III cells (73%), and smaller fractions of type II (24%) and type I cells (3%), similar to the pattern seen for wild-type prestin (Fig. 4b). Thus, deletion of more than 35 C-terminal amino acids results in impaired delivery of prestin to the PM and consequent elimination of NLC function.

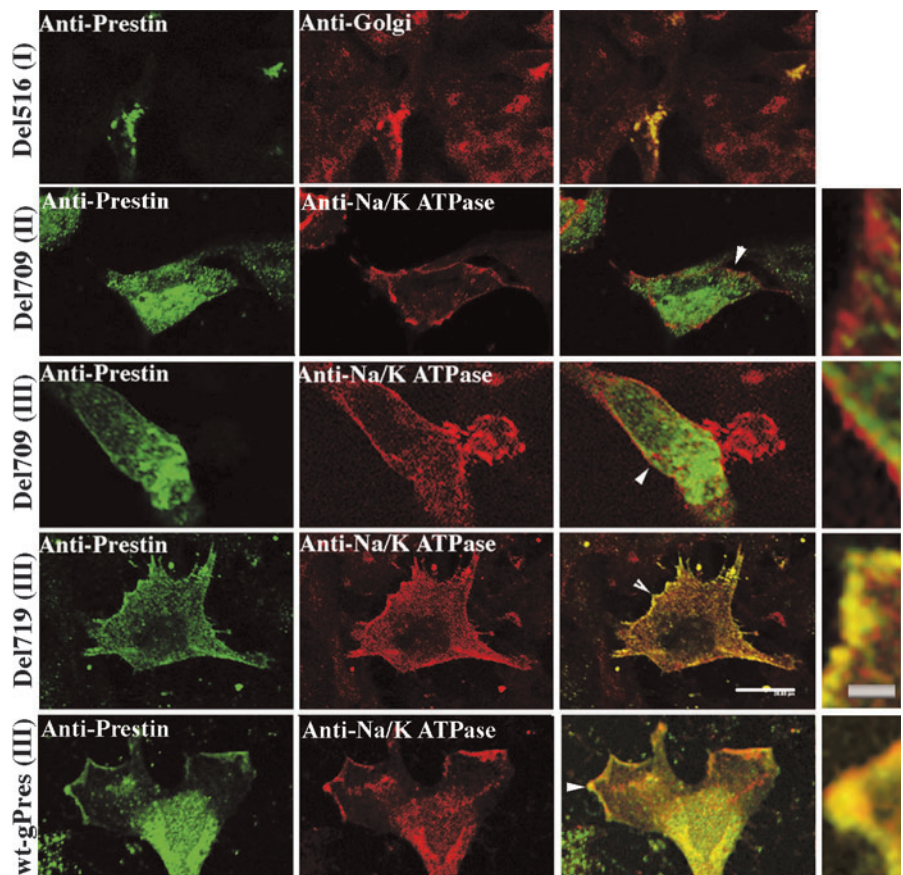
#### Subcellular locations of prestin and mutant proteins

The expression patterns of Del516, Del525, Del590, Del630, Del709 and Del719 were more closely examined by co-localization of prestin with other subcellular component markers:  $\text{Na}^+/\text{K}^+$  ATPase as a plasma-membrane marker and Golgin 97 detected with anti-golgin 97 Ab served as a Golgi-complex marker. These markers were tagged with red Rhodamine, while prestin was labeled with anti-N-mPres combined with green FITC tag. As we described above, mutants Del516, Del525 and Del590 resulted in prestin-expressing cells

with mostly a type I pattern (Fig. 4). As shown in the upper row of Fig. 5 (Del516, type I), the dense, punctate green prestin staining in the perinuclear region of the cell co-localized with the red Golgi marker, resulting in a yellow image when green and red images were superimposed as seen in the third column. The yellow image indicates that in type I cells prestin remained in the Golgi. The type II pattern was seen mainly with Del630 and Del709. The images from Del709 are shown as an example of the type II cells found in all mutants. The green staining (prestin) in type II cells was spread through the cytoplasmic region, including the Golgi (double labeling with Golgi marker is not shown here). However, prestin did not insert into the PM in type II cells as demonstrated in the second row of Fig. 5. The red staining of the PM marker ( $\text{Na}^+/\text{K}^+$  ATPase) is seen to be peripheral to the green prestin labeling distributed in focal staining throughout the cytoplasm. This can best be seen in the higher magnification image of the cell boundary (indicated by arrow) in the far right column.

Del709 had the largest percentage of type III cells (10%) of the truncation mutants lacking NLC. To determine whether the prestin protein was truly inserted into the plasma membrane of the cells classified as type III from the Del709 transfection, we examined its co-localization with  $\text{Na}^+/\text{K}^+$  ATPase, a plasma membrane protein made naturally by OK cells. As shown in the third row of Fig. 5, the cells classified as type III of Del709 do not appear to have the protein inserted into the plasma membrane. The enlarged image (far right) shows that the  $\text{Na}^+/\text{K}^+$  ATPase staining (red) was localized peripheral to the Del709 protein (green). Consequently, it appears that those cells defined as type III for Del709, without the use of a PM

**Fig. 5.** Subcellular localization of prestin and mutant proteins in type I, II and III cells. Immunofluorescence images of OK cells transiently transfected with wild type (wt-gPres) and three deletion mutants: Del516, Del709 and Del719. Three morphological phenotypes: types I, II and III are indicated for each mutant-expressing cell on the left side of the images. Red: anti-Golgi or anti- $\text{Na}^+/\text{K}^+$  ATPase markers.  $\text{Na}^+/\text{K}^+$  ATPase is a plasma-membrane protein. Green: FITC-labeled anti-N-mPres, which indicates the location of prestin. Yellow images are superimposed from green and red images, indicating the co-localization of prestin and  $\text{Na}^+/\text{K}^+$  ATPase or Golgi marker in the cell's plasma membrane or intracellular membranes. For better examination of the co-localization of prestin with the red markers, the images of the far right column are given at higher magnification. These segments correspond to the locations marked with white arrows. Note that in type II cells (example: Del709) the two labels are very close, but do not superimpose. Similarly, in some cells classified as type III, the two markers form parallel, adjacent, but not overlapping layers. In other cells, classified as type III (wild type and Del719), there is clear overlap, indicated by yellow color. Images were taken 48 hours after transfection. Bar, 20  $\mu\text{m}$ .



marker, do not in fact have prestin inserted in the PM. By contrast, Del719 (the fourth row of Fig. 5) demonstrates near complete co-localization in the PM with  $\text{Na}^+/\text{K}^+$  ATPase (yellow image), similar to the wild type as shown in the lowest row of Fig. 5. We have defined co-localization of prestin and  $\text{Na}^+/\text{K}^+$  ATPase by the presence of yellow staining in the merged images of prestin localization and  $\text{Na}^+/\text{K}^+$  ATPase localization. This co-localization is not quantitative, as different antibodies are used for detection of each of the proteins. Although, a yellow color is present in the merged images, we have no biochemical information on the structural relationship between membrane-expressed prestin and  $\text{Na}^+/\text{K}^+$  ATPase. A result identical to that of the co-localization of prestin and  $\text{Na}^+/\text{K}^+$  ATPase was obtained using the GHRH receptor (data not shown). GHRH receptor is a G-protein-coupled receptor expressed in the plasma membrane. These co-localization results indicate that all type I and II cells, and at least some of the cells classified as type III for Del709, lacked prestin localized to the PM. Therefore, type III cells expressing Del719 and wild type represent cells with successful PM insertion and demonstrable function of the protein. Thus, although Del709 expressing cells appear to produce 10% type III cells by our classification based on localization with only anti-N-mPres antibody, more refined experiments, using co-localization with  $\text{Na}^+/\text{K}^+$  ATPase demonstrate that the apposition of prestin to the membrane of Del709 is different from the true PM insertion seen in Del719 and wild type.

It is also worth mentioning that the proper localization of the  $\text{Na}^+/\text{K}^+$  ATPase and GHRH receptors, co-expressed with prestin proteins, indicates that the targeting defect seen is specific to the prestin mutants and does not result from a generalized disruption of cellular transport processes.

#### Prestin-pendrin (SLC26A4) and prestin-PAT1 (SLC26A6) chimeric proteins

Analysis of the deletion mutants demonstrated that we could only expect to detect NLC in cells in prestin mutants that possess the majority of the C-terminus; apparently necessary to accomplish proper PM targeting. In an attempt to produce a prestin truncation mutant that might retain the ability to localize to the PM, we made chimeric constructs by fusing C-terminal truncated forms of prestin with the analogous C-terminal portion of two closely related SLC26A proteins, pendrin (SLC26A4) and PAT1 (SLC26A6). Based on the availability of restriction sites and conserved amino acids in the STAS domain from the native sequences among these three SLC26A membranes, pendrin or PAT1 C-termini were fused with prestin at amino acids locations 515 or 644 to generate four chimera mutants: PRES/PDS-515 and PRES/PAT1-515, PRES/PDS-644 and PRES/PAT1-644. The 515 chimera replaces almost the entire C-terminus of prestin with the corresponding segment of either pendrin or Pat1, while the 644 chimera replaces part of the STAS domain, maintaining the original charge domains of prestin.

All chimeras displayed similar patterns of intracellular expression, with a predominance of type II cells as opposed to type III cells (wild-type prestin). By contrast, the corresponding prestin deletions Del516 and Del630 produced approximately 95% and 49% type I phenotypes respectively (Fig. 6). After adding the C-terminus from PDS or PAT1, the

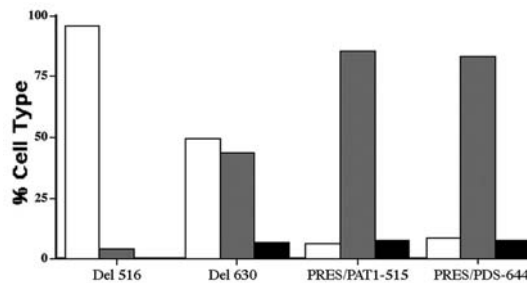


**Fig. 6.** Distribution of type I, II and III cells for the two chimeric and two deletion mutants. Deletion mutants close to the fusion sites are shown for comparison. White indicates type I cells, gray type II cells, and black type III cells.

pattern shifted to dominant type II (more than 83%). A similar shift from type I to type II occurred with PRES/PDS-644 and PRES/PAT1-644 when compared with Del630 (Fig. 4). Del630 showed 49% type I and 44% type II cells. After adding the C-terminus from PDS or PAT1, PRES/PDA-644 has 9% of type I, 83% of type II and 8% of type III cells. In other words, deletions produce mostly type I, while corresponding chimeras make type II phenotypes.

Furthermore, none of the chimeric constructs had measurable NLC (data not shown). These constructs were tested using the same methods as for the deletion constructs. TSA-201 cells were transiently transfected with chimera constructs and incubated between 24 and 48 hours. A set of positive control cells was transfected with wild type together with the experimental constructs. After incubation, cells transfected with the chimeric construct were dissociated and voltage clamped in the whole-cell mode. Ionic-blocking solution, as described above, was used in the extracellular bath. Intracellular solution, composed as above, was used to fill the pipettes during recording. A sample of at least 10 cells was used per experiment to determine if the cell exhibited NLC. Data from cells that showed no demonstrable NLC were further compared with untransfected cells. Untransfected cells were selected from the same transiently transfected cell culture dish. In this context, lack of fluorescence flagged those cells that did not express the EGFP or prestin protein. Data from these untransfected cells were used as a negative control to which we compared seemingly flat experimental cells. There were no differences between the NLC of flat chimeric constructs and untransfected cells. In the same experiment, positive control cells (wild-type prestin expressing cells) demonstrated NLC as expected (data not shown). Thus, replacement of the C-terminus of prestin with the C-termini of two related proteins did not restore the electrophysiological function or plasma membrane targeting of prestin.

#### Site-directed mutagenesis

A caveat applies to the interpretation of results obtained with chimeric proteins. Not only do the sequences of the transferred analogous portions of the C-terminus of pendrin and PAT1 have low homology to prestin, they also have different lengths compared with prestin's C-terminus. Furthermore, pendrin and PAT1 are expressed in the apical membranes of polarized epithelial cells. Pendrin is located in the apical membranes of several epithelial cell types, including those in thyroid (Royaux

et al., 2000), kidney (Royaux et al., 2001) and ear (Royaux et al., 2003). PAT1 is expressed in the apical surface of cells in renal proximal tubules (Knauf et al., 2001), the apical membranes of epithelial cells in the duodenum (Wang et al., 2002), collecting ducts (Petrovic et al., 2003) and pancreatic ductal cells (Lohi et al., 2000). Prestin, however, is expressed in the highly specialized lateral membranes of OHCs (Belyantseva et al., 2000; Zheng et al., 2001), which are also polarized epithelial cells. Since the chimera mutants (PRES/PDS and PRES/PAT1) could not restore prestin's PM targeting, we suspected that the capacity for prestin to insert into the PM of cultured epithelial cells is dependent on prestin-specific C-terminal amino acid residues.

A tyrosine-containing motif (YXX $\phi$ ) is one of several well-studied motifs that direct the transport of newly synthesized membrane protein from the trans-Golgi network to the basolateral membrane (BLM) (Keller and Simons, 1997). In this motif, Y is tyrosine, X is any amino acid, and  $\phi$  is a bulky hydrophobic amino acid. There are seven potential tyrosine-containing motifs in the C-terminus of prestin. The aberrant PM targeting seen with the deletion mutants and chimeric proteins may be related to the loss of potential BLM targeting motifs located in the C-terminus. To approach the question whether these motifs might be involved in membrane targeting of prestin to its PM location, we created a double point mutant: Y520A/Y526A, which abolished two of the seven potential tyrosine-containing motifs.

Previously, it has been established that wild type and a gprestin-EGFP fusion protein with a C-terminal EGFP extension, have similar subcellular distribution and electrophysiologic function (Ludwig et al., 2001). Consequently, double point mutants were generated from gprestin-EGFP to allow for immediate direct localization *via* fluorescence. The expression patterns of the targeting-motif mutants were observed 24 hours after transfection (Fig. 7). Control cells, expressing wild-type prestin, demonstrated co-localization with Na<sup>+</sup>/K<sup>+</sup> ATPase, similar to the lowest panel in Fig. 5. The mutation Y520A/Y526A resulted in intracellular accumulation of prestin in a type I and II pattern, and produced no co-localization with Na<sup>+</sup>/K<sup>+</sup> ATPase (Fig. 7, lower row) or with an alternative PM

marker, GHRH receptor (data not shown). Y520A/Y526A also lacked NLC as shown in Fig. 2. In contrast to the tyrosine targeting motif mutants, an adventitiously produced double mutant, V499G/Y501H, was able to insert into the PM, similar to the wild-type prestin (Fig. 7, upper panel). We note that Y501 is not a part of some potential membrane-targeting tyrosine motif, inasmuch as there is no requisite bulky hydrophobic amino acid at the 504 site. The mutation V499G/Y501H abolishes a pair of hydrophobic residues near transmembrane domain 12 as shown in Fig. 1. Although V499G/Y501H fully inserted into the PM of the cells (Fig. 7, upper row), this mutant had lost its NLC function (data not shown).

## Discussion

The C-terminus of prestin is the least well-conserved region compared with other SLC26A proteins and it contains some unusual features, as noted in the Introduction. Oliver and colleagues (Oliver et al., 2001), Santos-Sacchi's group (Santos-Sacchi, 2003) and our own work (Deák et al., 2005) have demonstrated that mutations of certain charged amino acids in the C-terminus of prestin can modify, but not eliminate, its voltage sensitivity. Since replacement of numerous charged amino acids in the C-terminus was not able to abolish NLC, and did not disrupt PM targeting (Oliver et al., 2001), we used serial deletions, site-directed mutagenesis and chimeric proteins, so that the structural features of the C-terminus could be examined in some detail.

The mutants Del516, Del525 and Del590 all lost NLC and showed prestin localization consistent with retention of the protein in ER and Golgi apparatus of the cells (type I). Del630, which retains both charge-cluster groups, also lacked NLC, and displayed near equal amounts of type I and type II cell patterns. The latter cell type, aside from ER and Golgi staining, displayed widespread cytoplasmic membranous staining without apparent PM localization. This suggests that the region of prestin between amino acids 590 and 630 is necessary for prestin to exit from the ER/Golgi into cytoplasmic vesicles. This failure to exit the Golgi by the truncated forms of prestin is likely the result of improper folding of the mutants (Ellgaard and Helenius, 2003), a phenomenon commonly seen with mutated membrane proteins. The mutants Del709 and Del719 have a dominant expression pattern of type II and type III respectively. Del719 is the only deletion mutant that retains NLC function. The pattern of cellular distribution of the deletion mutants thus correlated with the NLC function of the proteins. Normal NLC was seen only in transfections of mutant proteins that resulted in a majority of type III cells, consistent with type III cells having PM localization.

In an attempt to restore PM targeting in the truncation mutants, a set of chimeric prestin constructs were created in which the analogous C-terminus portions of PAT1 or PDS, the two most closely related proteins to prestin, were exchanged for the prestin C-terminus at sites of 515 and 644. The '515' chimera replaced almost the entire C-terminus of prestin with either pendrin or Pat1, while '646' chimera replaced part of the STAS domain. All chimeric proteins lacked NLC, and had altered cellular distribution, with a majority of cells of type II phenotype (more than 83%), instead of a majority type I cells (95%) with Del516 and 49% type I with Del630. Thus, adding the analogous C-terminus from other SLC26A family members

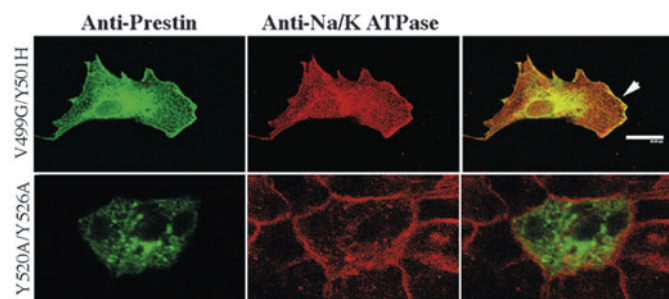


**Fig. 7.** Immunofluorescence images of OK cells transiently transfected with double point mutants: V499G/Y501H and Y520A/Y526A. Red, anti-Na<sup>+</sup>/K<sup>+</sup> ATPase; green, prestin with EGFP attached to its C-terminus. Yellow images are superimposed from green and red images, indicating the co-localization of prestin and Na<sup>+</sup>/K<sup>+</sup> ATPase in the cell's plasma membrane indicated by the arrow. There is no co-localization of prestin with the PM marker for Y520A/Y526A. Images were taken 24 hours after transfection. Bar, 20  $\mu$ m.



did have an effect on cellular processing of prestin, but this was different from that caused by prestin truncations that most closely corresponded to the chimeric protein junction points. The donor C-termini appear to have given the chimeric proteins the ability to exit from the ER/Golgi and become type II cells. However, the ability of prestin to insert into the PM appears dependent on prestin-specific C-terminus amino acid sequences. This observation and the aberrant PM expression seen with the potential BLM targeting-motif mutant (Y520A/Y526A) both suggest that unique amino acid sequence of the C-terminus determines the cellular distribution of prestin. A similar observation has also been reported recently based on truncated and chimeric constructs of Arabidopsis sulfate transporters, where the C-terminus, including a STAS domain, was suggested to be important for accumulation of the sulfate transporter in the plasma membrane (Shibagaki and Grossman, 2004).

A comparison of Del709 and Del719 is particularly revealing. Del709 lacks NLC and Del719 retains NLC function. Similar results showed that Del705 loses its NLC, while Del724 retains its normal NLC function (Bai et al., 2003). As shown in Figs 4 and 5, Del709 has a widespread cytoplasmic membranous staining (type II), while Del719 had wild type (type III) cellular distribution. This indicates that amino acids between 709 and 719 are required for proper PM targeting and that a truncation of 35 amino acids of prestin's C-terminus is able to eliminate proper membrane targeting. Recently, a comparable result was also discovered in the rat sulfate anion transporter sat-1 (SLC26A1), where deletion between the last 3 and 30 residues led to aberrant intracellular expression (Regeer and Markovich, 2004). However, not all SLC26A members need their distal C-terminal sequence for proper membrane targeting. For example, the PAT1 isoform, SLC26A6d, which lacks the last ~80 amino acids, was expressed in the PM and performed its anion transport function (Lohi et al., 2000). It is possible that the distal C-terminal sequence required for the PM targeting is limited to proteins targeted to the BLM, such as sat-1 and prestin.

How the distal amino acids of the C-terminus regulate PM targeting is not understood. In our studies, the mutant Y520A/Y526A resulted in type II morphology, suggesting that membrane targeting is not simply dependent on the mere presence of the distal C-terminal sequence, but rather may be dependent on a specific sequence in prestin. The distal C-terminal sequence is necessary but not sufficient for proper PM targeting or expression of NLC of transfected prestin. A complex system, involving multiple motifs, is likely to affect prestin's membrane targeting. The tyrosine and di-leucine motifs are two well-studied motifs involved in BLM targeting (Keller and Simons, 1997). There are seven potential tyrosine-containing motifs and two di-leucine motifs in the C-terminus of prestin. The function of each of these motifs needs further investigation in polarized epithelial cells. Alternatively, the failure of the double mutant Y520A/Y526A to achieve membrane expression might simply be due to the misfolding of the mutant protein and subsequent failed transport to the PM. Nevertheless, our data demonstrate that alteration of two potential BLM targeting motifs disrupts the localization of prestin. Whether one or both of the tyrosine residues at amino acids 520 and 526 act as a BLM targeting motif needs further investigation in polarized epithelial cells.

Pendrin, DTDST and DRA are the best characterized of the SLC26A proteins because of their prominent phenotype when mutated in humans. Many of the disease-causing mutations occur in the C-termini of these proteins. The majority of these mutant proteins have improper PM targeting and loss of some or full function. Certain *PDS* mutations result in a phenotype of Pendred's syndrome (deafness and a hypothyroid goiter), others produce the clinical syndrome associated with DFNB4 (deafness and dilated vestibular aqueducts, without goiter). In general, pendrin mutant proteins, which completely abolish PM targeting and/or function, result in Pendred's syndrome, while other mutations, which retain some PM targeting and residual function, result in a DFNB4 phenotype (Scott et al., 2000). Mutation of the *DTDST* gene produces a wide variety of skeletal diseases, but there is no obvious pattern to the mutant location and phenotype produced. The mutations of *prest*, which resulted in a type I and II morphology, represent proteins retained in the ER/Golgi and/or cytoplasmic vesicles. The results presented here are very similar to some of the well-characterized human mutations of *PDS*, which show altered protein localization (Rotman-Pikielny et al., 2002; Taylor et al., 2002). It would therefore appear that multiple members of the SLC26A family of proteins are dependent on specific, but not identical, sequences in their C-termini for both PM targeting and function.

The double mutant V499G/Y501H produced a protein that was efficiently delivered to the PM, but which completely lacked NLC. Since we know nothing about prestin's membrane stoichiometry, three-dimensional structure, and very little about its anion-binding site, the mechanism whereby this mutant affects prestin's function is unknown. It may interfere with voltage-regulated anion binding, or the consequent conformational change of the protein. Our observations indicate that specific sequences within the C-terminus are essential for the NLC function in addition to its role in membrane targeting. While PM delivery is obviously necessary, it is not a sufficient condition for prestin function. The C-terminus of prestin is likely to be intimately involved in anion binding, membrane targeting, and the voltage regulated conformational change of prestin.

We are grateful to Haitao Wen, Donald E. Robison and Kevin Long for contributing to some of the molecular biological experiments. We thank W. Russin at the Biological Imaging Facility of Northwestern University for his help in image processing, Kelly Mayo of Northwestern University for providing the GHRH receptor construct, and Jian Zuo of the St Jude Children's Hospital for providing prestin-knockout mice. This work is supported by the National Institutes of Health, NIDCD, DC00089.

## References

- Ashmore, J. F. (1987). A fast motile response in guinea-pig outer hair cells: the cellular basis of the cochlear amplifier. *J. Physiol.* **388**, 323-347.
- Ashmore, J. F. (1990). Forward and reverse transduction in the mammalian cochlea. *Neurosci. Res. (Suppl.)* **12**, S39-S50.
- Bai, J. B., Samaranayake, H. S., Navaratnam, D. S. and Santos-Sacchi, J. (2003). Carboxy-terminal truncations and mutations of prestin; affects on NLC. *Assoc. Res. Otolaryngol. Abs.*: 1871.
- Belyantseva, I. A., Adler, H. J., Curi, R., Frolenkov, G. I. and Kachar, B. (2000). Expression and localization of prestin and the sugar transporter GLUT-5 during development of electromotility in cochlear outer hair cells. *J. Neurosci.* **20**, RC116.
- Brownell, W. E., Bader, C. R., Bertrand, D. and de Ribaupierre, Y. (1985). Evoked mechanical responses of isolated cochlear outer hair cells. *Science* **227**, 194-196.

- Chambard, J. M. and Ashmore, J. F.** (2003). Sugar transport by members of the SLC26 superfamily of anion-bicarbonate exchangers. *J. Physiol.* **550**, 667-677.
- Cheatham, M. A., Huynh, K. H., Gao, J., Zuo, J. and Dallos, P.** (2004). Cochlear function in prestin knockout mice. *J. Physiol.* **560**, 821-830.
- Dallos, P.** (1992). The active cochlea. *J. Neurosci.* **12**, 4575-4585.
- Dallos, P.** (1996). Overview: cochlear neurophysiology. In *The Cochlea (Springer Handbook of Auditory Research)* (ed. P. Dallos, A. N. Popper and R. R. Fay), pp. 1-43. New York: Springer.
- Dallos, P. and Fakler, B.** (2002). Prestin, a new type of motor protein. *Nat. Rev. Mol. Cell Biol.* **3**, 104-111.
- Deák, L., Zheng, J., Orem, A., Du, G. G., Aguiñaga, S., Matsuda, K. and Dallos, P.** (2005). Effects of cyclic nucleotides on the function of prestin. *J. Physiol.* **563**, 483-496.
- Ellgaard, L. and Helenius, A.** (2003). Quality control in the endoplasmic reticulum. *Nat. Rev. Mol. Cell Biol.* **4**, 181-191.
- Everett, L. A. and Green, E. D.** (1999). A family of mammalian anion transporters and their involvement in human genetic diseases. *Hum. Mol. Genet.* **8**, 1883-1891.
- Everett, L. A., Morsli, H., Wu, D. K. and Green, E. D.** (1999). Expression pattern of the mouse ortholog of the Pendred's syndrome gene (Pds) suggests a key role for pendrin in the inner ear. *Proc. Natl. Acad. Sci. USA* **96**, 9727-9732.
- Hastbacka, J., Superti-Furga, A., Wilcox, W. R., Rimoin, D. L., Cohn, D. H. and Lander, E. S.** (1996a). Atelosteogenesis type II is caused by mutations in the diastrophic dysplasia sulfate-transporter gene (DTDST): evidence for a phenotypic series involving three chondrodysplasias. *Am. J. Hum. Genet.* **58**, 255-262.
- Hastbacka, J., Superti-Furga, A., Wilcox, W. R., Rimoin, D. L., Cohn, D. H. and Lander, E. S.** (1996b). Sulfate transport in chondrodysplasia. *Ann. New York Acad. Sci.* **785**, 131-136.
- Holley, M. C.** (1996). Outer hair cell motility. In *The Cochlea (Springer Handbook of Auditory Research)* (ed. P. Dallos, A. N. Popper and R. R. Fay), pp. 386-434. New York: Springer.
- Jones, D. T.** (1999). Protein secondary structure prediction based on position-specific scoring matrices. *J. Mol. Biol.* **292**, 195-202.
- Kachar, B., Brownell, W. E., Altschuler, R. and Fex, J.** (1986). Electrokinetic shape changes of cochlear outer hair cells. *Nature* **322**, 365-368.
- Keller, P. and Simons, K.** (1997). Post-Golgi biosynthetic trafficking. *J. Cell Sci.* **110**, 3001-3009.
- Kere, J., Lohi, H. and Høglund, P.** (1999). Genetic disorders of membrane transport III. Congenital chloride diarrhea. *Am. J. Physiol.* **276**, G7-G13.
- Knauf, F., Yang, C. L., Thomson, R. B., Mentone, S. A., Giebisch, G. and Aronson, P. S.** (2001). Identification of a chloride-formate exchanger expressed on the brush border membrane of renal proximal tubule cells. *Proc. Natl. Acad. Sci. USA* **98**, 9425-9430.
- Lieberman, M. C., Gao, J., He, D. Z., Wu, X., Jia, S. and Zuo, J.** (2002). Prestin is required for electromotility of the outer hair cell and for the cochlear amplifier. *Nature* **419**, 300-304.
- Liu, X. Z., Ouyang, X. M., Xia, X. J., Zheng, J., Pandya, A., Li, F., Du, L. L., Welch, K. O., Petit, C., Smith, R. J. et al.** (2003). Prestin, a cochlear motor protein, is defective in non-syndromic hearing loss. *Hum. Mol. Genet.* **12**, 1155-1162.
- Lohi, H., Kujala, M., Kerkela, E., Saarialho-Kere, U., Kestila, M. and Kere, J.** (2000). Mapping of five new putative anion transporter genes in human and characterization of SLC26A6, a candidate gene for pancreatic anion exchanger. *Genomics* **70**, 102-112.
- Loughlin, P., Shelden, M. C., Tierney, M. L. and Howitt, S. M.** (2002). Structure and function of a model member of the SulP transporter family. *Cell Biochem. Biophys.* **36**, 183-190.
- Ludwig, J., Oliver, D., Frank, G., Klocker, N., Gummer, A. W. and Fakler, B.** (2001). Reciprocal electromechanical properties of rat prestin: the motor molecule from rat outer hair cells. *Proc. Natl. Acad. Sci. USA* **98**, 4178-4183.
- Matsuda, K., Zheng, J., Du, G. G., Klocker, N., Madison, L. D. and Dallos, P.** (2004). N-linked glycosylation sites of the motor protein prestin: effects on membrane targeting and electrophysiological function. *J. Neurochem.* **89**, 928-938.
- McGuffin, L. J., Bryson, K. and Jones, D. T.** (2000). The PSIPRED protein structure prediction server. *Bioinformatics* **16**, 404-405.
- Mount, D. B. and Romero, M. F.** (2004). The SLC26 gene family of multifunctional anion exchangers. *Pflug. Arch.* **447**, 710-721.
- Oliver, D., He, D. Z., Klocker, N., Ludwig, J., Schulte, U., Waldegger, S., Ruppertsberg, J. P., Dallos, P. and Fakler, B.** (2001). Intracellular anions as the voltage sensor of prestin, the outer hair cell motor protein. *Science* **292**, 2340-2343.
- Petrovic, S., Wang, Z., Ma, L. and Soleimani, M.** (2003). Regulation of the apical Cl<sup>-</sup>/HCO<sub>3</sub><sup>-</sup> exchanger pendrin in rat cortical collecting duct in metabolic acidosis. *Am. J. Physiol. Renal Physiol.* **284**, F103-112.
- Regeer, R. R. and Markovich, D.** (2004). A dileucine motif targets the sulfate anion transporter sat-1 to the basolateral membrane in renal cell lines. *Am. J. Physiol. Cell Physiol.* **287**, C365-C372.
- Rotman-Pikielny, P., Hirschberg, K., Maruvada, P., Suzuki, K., Royaux, I. E., Green, E. D., Kohn, L. D., Lippincott-Schwartz, J. and Yen, P. M.** (2002). Retention of pendrin in the endoplasmic reticulum is a major mechanism for Pendred syndrome. *Hum. Mol. Genet.* **11**, 2625-2633.
- Royaux, I. E., Suzuki, K., Mori, A., Katoh, R., Everett, L. A., Kohn, L. D. and Green, E. D.** (2000). Pendrin, the protein encoded by the Pendred syndrome gene (PDS), is an apical porter of iodide in the thyroid and is regulated by thyroglobulin in FRTL-5 cells. *Endocrinology* **141**, 839-845.
- Royaux, I. E., Wall, S. M., Karniski, L. P., Everett, L. A., Suzuki, K., Knepper, M. A. and Green, E. D.** (2001). Pendrin, encoded by the Pendred syndrome gene, resides in the apical region of renal intercalated cells and mediates bicarbonate secretion. *Proc. Natl. Acad. Sci. USA* **98**, 4221-4226.
- Royaux, I. E., Belyantseva, I. A., Wu, T., Kachar, B., Everett, L. A., Marcus, D. C. and Green, E. D.** (2003). Localization and functional studies of pendrin in the mouse inner ear provide insight about the etiology of deafness in pendred syndrome. *J. Assoc. Res. Otolaryngol.* **4**, 394-404.
- Rybalchenko, V. and Santos-Sacchi, J.** (2003). Cl<sup>-</sup> flux through a non-selective, stretch-sensitive conductance influences the outer hair cell motor of the guinea-pig. *J. Physiol.* **547**, 873-891.
- Saier, M. H.** (1999). Genome archeology leading to the characterization and classification of transport proteins. *Curr. Opin. Microbiol.* **2**, 555-561.
- Santos-Sacchi, J.** (1991). Reversible inhibition of voltage-dependent outer hair cell motility and capacitance. *J. Neurosci.* **11**, 3096-3110.
- Santos-Sacchi, J.** (2003). New tunes from Corti's organ: the outer hair cell boogie rules. *Curr. Opin. Neurobiol.* **13**, 459-468.
- Scott, D. A., Wang, R., Kreman, T. M., Andrews, M., McDonald, J. M., Bishop, J. R., Smith, R. J., Karniski, L. P. and Sheffield, V. C.** (2000). Functional differences of the PDS gene product are associated with phenotypic variation in patients with Pendred syndrome and non-syndromic hearing loss (DFNB4). *Hum. Mol. Genet.* **9**, 1709-1715.
- Shibagaki, N. and Grossman, A. R.** (2004). Probing the function of STAS domains of the Arabidopsis sulfate transporters. *J. Biol. Chem.* **279**, 30791-30799.
- Soleimani, M., Greeley, T., Petrovic, S., Wang, Z., Amlal, H., Kopp, P. and Burnham, C. E.** (2001). Pendrin: an apical Cl<sup>-</sup>/OH<sup>-</sup>/HCO<sub>3</sub><sup>-</sup> exchanger in the kidney cortex. *Am. J. Physiol. Renal Physiol.* **280**, F356-F364.
- Superti-Furga, A., Hastbacka, J., Rossi, A., van der Harten, J. J., Wilcox, W. R., Cohn, D. H., Rimoin, D. L., Steinmann, B., Lander, E. S. and Gitzelmann, R.** (1996a). A family of chondrodysplasias caused by mutations in the diastrophic dysplasia sulfate transporter gene and associated with impaired sulfation of proteoglycans. *Ann. New York Acad. Sci.* **785**, 195-201.
- Superti-Furga, A., Hastbacka, J., Wilcox, W. R., Cohn, D. H., van der Harten, H. J., Rossi, A., Blau, N., Rimoin, D. L., Steinmann, B., Lander, E. S. et al.** (1996b). Achondrogenesis type IB is caused by mutations in the diastrophic dysplasia sulphate transporter gene. *Nat. Genet.* **12**, 100-102.
- Superti-Furga, A., Rossi, A., Steinmann, B. and Gitzelmann, R.** (1996c). A chondrodysplasia family produced by mutations in the diastrophic dysplasia sulfate transporter gene: genotype/phenotype correlations. *Am. J. Med. Genet.* **63**, 144-147.
- Taylor, J. P., Metcalfe, R. A., Watson, P. F., Weetman, A. P. and Trembath, R. C.** (2002). Mutations of the PDS gene, encoding pendrin, are associated with protein mislocalization and loss of iodide efflux: implications for thyroid dysfunction in Pendred syndrome. *J. Clin. Endocrinol. Metab.* **87**, 1778-1784.
- Wang, Z., Petrovic, S., Mann, E. and Soleimani, M.** (2002). Identification of an apical Cl<sup>-</sup>/HCO<sub>3</sub><sup>-</sup> exchanger in the small intestine. *Am. J. Physiol.* **282**, G573-G579.
- Zheng, J., Shen, W., He, D. Z., Long, K. B., Madison, L. D. and Dallos, P.** (2000). Prestin is the motor protein of cochlear outer hair cells. *Nature* **405**, 149-155.
- Zheng, J., Long, K. B., Shen, W., Madison, L. D. and Dallos, P.** (2001). Prestin topology: localization of protein epitopes in relation to the plasma membrane. *NeuroReport* **12**, 1929-1935.